

Lifetime of the 937- and 885-keV resonances in the $^{27}\text{Al}(p, \alpha)$ reaction

F. Malaguti, A. Uguzzoni, and E. Verondini

*Istituto Nazionale di Fisica Nucleare—Sezione di Bologna
and Istituto di Fisica dell'Università, Bologna, Italy*

(Received 14 November 1978)

We have used the crystal blocking technique to measure the lifetimes of ^{28}Si compound states excited by the $^{27}\text{Al}(p, \alpha)$ reaction at $E_p = 937$ and 885 keV. Axial blocking on the $\langle 110 \rangle$ axis of thick Al crystals and Kodak LR 115 plastic detectors are used. Measurements have been made at a $0.2 \mu\text{m}$ depth. A study is made of the yields of some (p, α) resonances on Al and of the depth dependence of blocking dips. The data are analyzed by comparison with a realistic Monte Carlo model. The resulting lifetime, $\tau_{937} < 17$ as (as $= 10^{-18}$ s) and $\tau_{885} = 38_{-9}^{+10}$ as are compared with previous work.

NUCLEAR REACTIONS $^{27}\text{Al}(p, \alpha)^{24}\text{Mg}$, $E = 0.731 - 1.183$ MeV; measured yields in thin targets. LR 115 cellulose nitrate detectors. $E = 0.885, 0.937$ MeV; measured blocking effect. ^{28}Si deduced mean lifetime. Single crystal thick Al targets.

I. INTRODUCTION

The crystal blocking method for measuring nuclear lifetimes is now becoming a well-established experimental technique¹ and does not need more than a schematic description such as that shown in Fig. 1.

The measurements on isolated resonances are particularly simple because they are free from complications due to multilevel effects (e.g., level-level correlations) and the possible resulting nonexponential decay of the compound system.² If, moreover, the lifetimes of these resonances are known by some other way, the measurements can be used as a general check of the method.³

We report here measurements on two resonances in the $^{27}\text{Al}(p, \alpha)^{24}\text{Mg}$ reaction, occurring at $E_p = 937$ and 885 keV and whose total width is already known.⁴ The 937-keV resonance has been studied by Nakayama *et al.*⁵ by planar blocking, and the 885-keV resonance by Alexander *et al.*⁶ both by planar and axial blocking. The results of the present experiment seem to be more accurate than the previous ones. We use here axial blocking in thick (≈ 2 mm) Al crystals. The beam energy is adjusted so as to have the reaction under study taking place at some $0.2 \mu\text{m}$ within the target.

Since the pileup due to back-scattered protons makes it impossible to use surface barrier counters, we use cellulose nitrate films to detect the α particles. Their energy resolution is very poor and this raises the problem of separating the α particles due to the reaction under study from those due to resonances at lower proton energies that are excited at larger depths within the targets. To do this, a particular study of the dependence of blocking dips on the emission depths has to be

made. For this and other auxiliary measurements the high-yield resonance at 1183 keV was exploited whose lifetime is too short⁴ to affect blocking dips.

II. EXPERIMENTAL DETAILS

A. Crystal preparation

The preparation of the crystals, their mounting on a goniometer with three degrees of freedom, and preliminary orientation by means of the x-ray Laue diffraction pattern have been described elsewhere.⁷ The only improvement with respect to Ref. 7 is that now we do not use any mechanical tool (such as a diamond saw, grit, polishing machine) to cut and to flatten the specimens, but only an electric spark cutting and polishing machine. This reduces substantially the mechanical stresses on the specimens, and leads to correspondingly higher quality of the final crystals, which are stored *in vacuo* to prevent surface contamination.

The quality of our crystals is shown by the "prompt" blocking dip in Fig. 2. The minimum yield χ_{min} is about 4% or less.

B. Experimental arrangement

The experimental setup is shown schematically in Fig. 3. The proton beam produced by the 2-MeV Van de Graaff generator of the INFN Laboratori Nazionali di Legnaro (Padua), after a double 1 mm collimation, impinges on the crystal at an angle of about 3° with respect to the $\langle 1\bar{1}0 \rangle$ axis to prevent channeling.

The "delayed" and "prompt" axial blocking dips are simultaneously recorded by D (delayed) and P (prompt) plastic detectors at angles 87° and 177° with respect to the beam. The blocking pattern on detector P serves as a reference, as the $\langle 1\bar{1}0 \rangle$

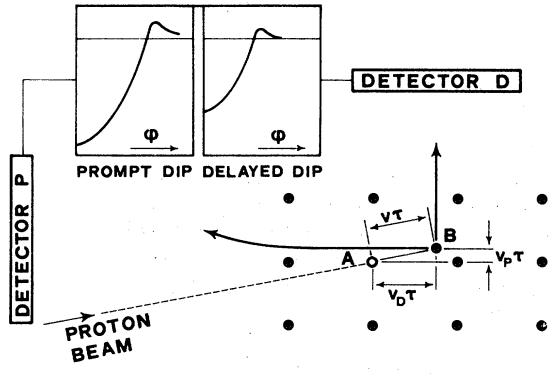


FIG. 1. Schematic representation of blocking lifetime measurements. *A* is the lattice position of the target nucleus, *B* the decay position of the compound nucleus. Two paths of "prompt" and "delayed" decay products are also schematically shown. ϕ is the angle between the crystal axis and the direction of the outgoing α particles.

axis is nearly parallel to the recoil direction and significant lifetime effects cannot be present. To prevent carbon contamination, the target is protected by a cold trap consisting of a hollow half-cylinder, with antiscatter baffles, whose axis is along the beam, terminating in a box surrounding the target with two holes in the direction of the detectors. The whole trap is made of copper cooled by conduction from liquid nitrogen outside the scattering chamber. To reduce losses by radiant heat,

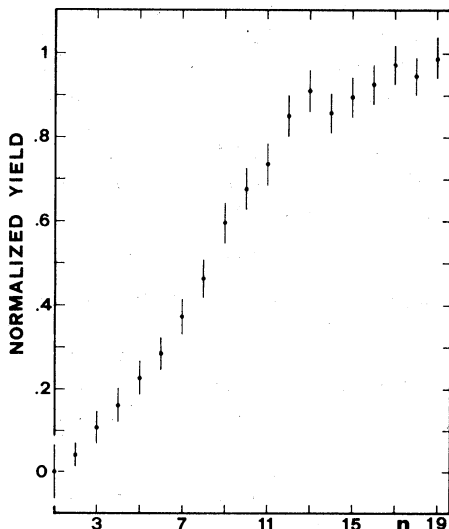


FIG. 2. A blocking dip of "prompt" α particles from the 1183-keV resonance at $\theta_{\text{lab}} = 176^\circ$. Beam dose = $348 \mu\text{C}$; current $\approx 200 \text{ nA}$ on a $\approx 1 \text{ mm}^2$ crystal area. The method of obtaining the dip is discussed in Sec. II C. *n* is the ordering number of 1-mrad circular rings around the dip center.

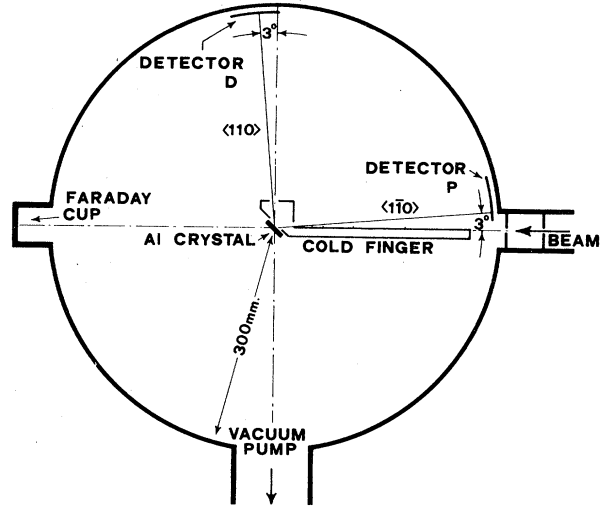


FIG. 3. Sketch of the experimental setup. Observe that the emission depth of the α particles is the same for the *D* and *P* detectors.

the trap is gold-plated.

A positive voltage of +90 V was applied to the crystal (or to the Faraday cup in some auxiliary measurements made with thin targets) to suppress secondary electrons and permit precise measurement of the beam charge.

C. The plastic detectors

The detectors *D* and *P* are Kodak LR 115 type I films. They consist of a $7 \mu\text{m}$ thick cellulose nitrate sheet strongly red-colored and coated on an inert polyester base. They are specially designed to record tracks of α particles with about 2-MeV energy. After 30–35 min etching in a 2.5 *N* solution of NaOH at 60°C , the tracks appear as small holes in the red sheet, which can be directly printed as black spots on a white background using a standard photographic enlarger and a green filter (Kodak Wratten No. 40) on the light beam. At about $15\times$ enlargement, the tracks are easily counted with the aid of a magnifying glass.

With respect to the celluloid sheets used previously,⁷ LR 115 has the advantage of being much easier to use and allows a safe discrimination between tracks and defects, even in the presence of a low track density.

In the conditions of the present experiment, no tracks due to the elastically scattered protons are seen in the final prints. They are, however, present in the original sheets as a very fine "granulation" and can be individually resolved using a $400\times$ microscope.

The area of interest in the prints is then divided into $5 \times 5 \text{ mm}^2$ squares, and the track number in

each square is stored and analyzed by a computer program⁷ which calculates the track density within circular rings corresponding to a 1 mrad angular width around the dip center. The isotropic counting rate used for normalization is determined by scanning a suitably chosen annular region of the print outside the dip. Planar effects are then averaged off. All the blocking dips reported here were obtained in this way. The corresponding figures show the normalized yield vs the ordering number n of the circular rings.

III. PRELIMINARY MEASUREMENTS

A. The yields of the resonances

The (p, α) resonances that are relevant in the present experiment occur at 1183, 937, 923, 885, 731, and 633 keV.⁴ Apart from the 633-keV resonance, their yields at the angles of interest ($\theta_{lab} = 87^\circ$ and 177°) have been measured using self-supporting evaporated Al targets ($\approx 0.35 \mu\text{m}$ thick). This permits the excitation of only one resonance at a time. The measured yields are reported in Table I. They can be considered as absolute assuming a 100% efficiency of the LR 115 detectors for ≈ 2 -MeV α particles. Quoted errors are only statistical and are significant only as far as the relative yields of different resonances are concerned. If the absolute yields are of interest, systematic errors will probably increase the uncertainties by a further 5% of the measured values.

B. Energy response of the detectors

The sensitivity of the LR 115 type I films to α particles with energies E between 0 and 2.3 MeV has been studied using the 937- and 1183-keV resonances and putting Mylar or aluminum absorbers of various thicknesses in front of the detectors. Assuming the efficiency to be 100% for 2.3-MeV α particles, we found that it remains 100% as far as ≈ 1 MeV, then it decreases reaching a constant value $\approx 30\%$ for $E \approx 500$ keV or less. We also observed that for $E \leq 700$ keV or less the etch pits are very small. Moreover, not all of them perforate the red film. With a suitable choice of the

TABLE I. Resonance yields.

Proton resonance energy in lab (keV)	Measured yield ($\alpha/\mu\text{C sr}$)	
	$\theta_{lab} = 87^\circ$	$\theta_{lab} = 177^\circ$
1183	$19\,500 \pm 350$	$20\,000 \pm 350$
937	$1\,800 \pm 20$	634 ± 12
923	118 ± 8	162 ± 7
885	412 ± 7	167 ± 4
731	235 ± 8	195 ± 6

etching and printing conditions, they give very pale images in the final print that can be easily discriminated from those produced by α particles with $E \geq 1$ MeV or more.

To summarize, the energy resolution of these detectors is very poor, but with some care it is possible to distinguish between α particles with $1 \text{ MeV} \leq E \leq 2.5 \text{ MeV}$ and those with $E \leq 700 \text{ keV}$. These conclusions are valid for the batch we used (No. VI 74.3, $7 \mu\text{m}$ thick red film) and should probably be revised for different ones.

C. Choice of the experimental conditions

The beam energy was chosen so that the resonance of interest takes place at a depth of some $0.2 \mu\text{m}$. Owing to the thickness of the target, at larger depths other resonances occur whose α particles can leave the crystal and reach the detectors. The situation for the two resonances studied in the present work is summarized in Table II as derived from known range-energy curves for protons and α particles in aluminum,⁸ with no corrections for channeling effects.

On the basis of Table II, we decided to perform the 937-keV measurement without absorbers in front of the detectors, since the α particles from the 731- and 633-keV resonances can be discriminated by a selective film printing and scanning; there is no hope of eliminating the α particles from the 923- and 885-keV ones, whose energies are too near to those being studied. Therefore, the 937-keV measurement was expected to contain contributions from the 923- and 885-keV resonances in the proportions given by Table I.

In contrast, the 885-keV experiment was performed with $4 \mu\text{m}$ thick Mylar foils on the detectors, which reduce the energy of the α particles from the 885- and 731-keV resonances to ≈ 1 and ≈ 0.1 MeV, respectively, and stop the α particles from the one at 633 keV.⁹ Therefore the 885-keV measurement was expected to be "clean."

These hypotheses were tested and found to be correct by comparing the results of separate

TABLE II. Depth of occurrence (D , in μm) of $^{27}\text{Al}(p, \alpha)^{24}\text{Mg}$ resonances and mean energies (\bar{E} , in MeV) of the α particles leaving the target at $\approx 90^\circ$ at the beam energies E_p used in this work.

Resonance	$E_p = 947 \text{ keV}$		$E_p = 895 \text{ keV}$		
	D	\bar{E}	Resonance	D	\bar{E}
937	0.2	2.08			
923	0.5	1.99			
885	1.2	1.76	885	0.2	2.05
731	4.1	≈ 0.7	731	3.1	1.08
633	5.7	≈ 0.1	633	4.7	≈ 0.5

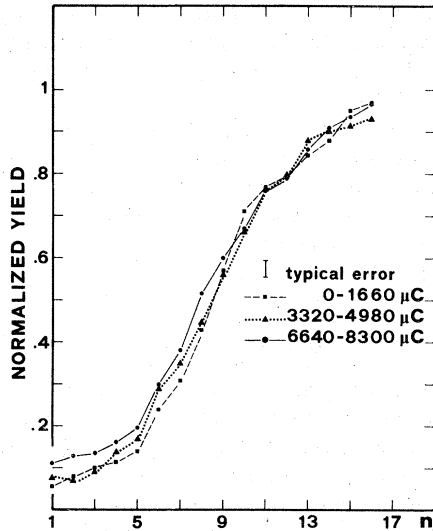


FIG. 4. Effect of radiation damage on blocking dips studied at $\theta_{\text{lab}} = 177^\circ$ with a beam current of 250 nA. $^{27}\text{Al}(p, \alpha)$, $E_p = 1183$ keV, $E_\alpha = 2.12$ MeV. n is the ordering number of 1-mrad circular rings around the dip center.

measurements on thick microcrystalline Al targets (and the isotropic counting rates on Al single crystals) with the numbers shown in Table I.

D. Radiation damage

A study of the radiation damage in the crystals was carried out using the "zero lifetime" 1183-keV resonance in order to determine the maximum admissible beam dose. The current was ≈ 250 nA

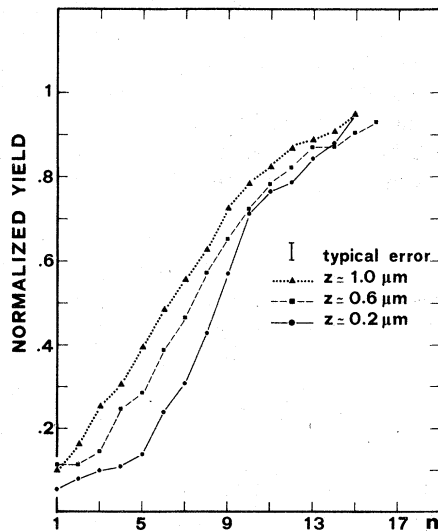


FIG. 5. Effect of emission depth z on blocking dips studied under similar conditions as in Fig. 4.

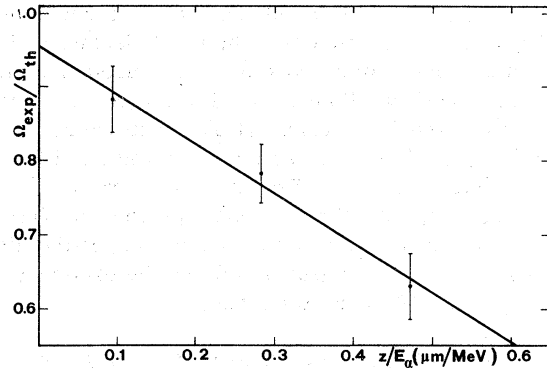


FIG. 6. Effect on emission depth z on dip volumes deduced from the data of Fig. 5. $\Omega_{\text{exp}}/\Omega_{\text{th}}$ is the ratio between measured and calculated volumes, while z/E_α is the ratio between depth and α -particles initial energy. The best fit line was found by χ^2 minimization.

on a ≈ 1 mm² area.

The result is shown in Fig. 4. It can be seen that under the present conditions a crystal of very good initial quality shows negligible radiation damage after a 8300 μC beam dose on the same area. This seems to be the limit since higher irradiation produces blistering of the surface (probably due to trapped hydrogen) that sometimes extends to the whole crystal.¹⁰

We decided to expose the same region of the target for not more than 6700 μC . Afterwards, in the long runs, the crystal was moved parallel to its surface and exposed in a new region provided that a preliminary check of quality and orientation had given satisfactory answers. The check can be performed using the 1183-keV resonance and the celluloid sheets described in Ref. 7 with a beam dose of ≈ 300 μC .

E. Depth effect

The dependence of α -particle blocking dips on the emission depth z has been studied using the 1183-keV resonance and adjusting the beam energy so that the reaction takes place at $z = 0.2, 0.6, 1$ μm . The dips observed are given in Fig. 5. Since the measurements were alternated with those of Fig. 4, there should be no significant contribution from radiation damage. It is interesting to observe that, as z increases, the dip becomes narrower while χ_{min} is affected only slightly.

As will be discussed in the next section, our main interest is in the dip volume Ω . Is it defined as

$$\Omega = 1 - D/S$$

where D and S are the counts within equal solid angles around the dip center (D) and in the iso-

tropic region (S).

The prompt dip volume calculated by the Monte Carlo program is $\Omega_{th} = 0.317 \pm 0.015$ for $z = 0.2 \mu\text{m}$ and $E_\alpha = 2.12 \text{ MeV}$, while that measured (see Fig. 5) is $\Omega_{exp} = 0.280 \pm 0.014$, 0.248 ± 0.013 , 0.200 ± 0.014 for 0.2, 0.6, 1.0 μm respectively. The volumes correspond to a cone of 17 mrad semi-aperture. Assuming a z/E_α dependence for the dip volumes,¹¹ the depth effect can be interpreted by giving Ω_{exp}/Ω_{th} as a function of z/E_α . This produces the three points and the best fit straight line shown in Fig. 6.

Hereafter we will assume that the linear dependence in Fig. 6 can be applied to different crystals, energies, and depths. Clearly this is only justifiable if all the crystals have similar qualities.

IV. METHOD OF ANALYSIS

A. Definition of the parameter R to be measured in a blocking lifetime experiment

Our method for analyzing blocking data uses the axial dip volume Ω that is reduced by the lifetime effect. Since the volume is also sensitive to multiple scattering and crystal defects we use the ratio $R = \Omega_D/\Omega_P$ between the delayed and prompt volumes. The reason for this is that R is less sensitive to multiple scattering and defects than Ω ; hence it provides a parameter independent of the properties of a particular crystal.¹²

For a given mean orthogonal displacement $v_\perp \tau$ of the compound nucleus from a crystal axis, the blocking dip shape and volume can be calculated by means of a multistring Monte Carlo program⁷ that takes into account the thermal vibrations of the lattice atoms and electronic multiple scattering. The α particles are assumed to be emitted at a depth of 0.2 μm , approximately that at which the reactions take place.

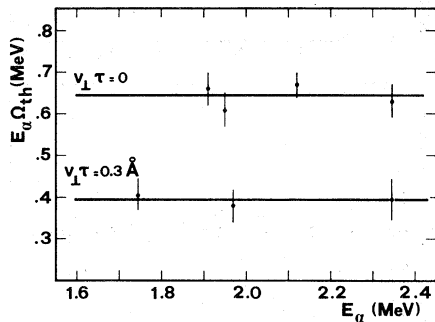


FIG. 7. Calculated products $E_\alpha \Omega_{th}$ vs E_α for $v_\perp \tau = 0$ and 30 pm. The α -particles energies E_α are within the range of interest in the present work. The zero slope best fit lines are also shown (see text).

Dip volumes depend on the energy of the blocked particles, because the steering effect of the atomic potential is weaker for more energetic ions.

Therefore, in the definition $R = \Omega_D/\Omega_P$ the volumes should be calculated for the appropriate α -particle energies that are different for each reaction and for the delayed and prompt dipo. The calculations can be greatly simplified if an analytical energy dependence of the dip volume is known. An important result of the single-string continuum model is that $\Omega \propto 1/E$,^{6,13} and we checked whether our Monte Carlo results obey the same law.

Figure 7 shows the products $E\Omega$ at four different energies for the same $v_\perp \tau = 0$ and at three different energies for $v_\perp \tau = 30 \text{ pm}$. Similar results have been obtained for different values of $v_\perp \tau$. The $E\Omega$ data appear to be consistent within the uncertainties arising from the Monte Carlo method, and it can be concluded that the law $\Omega \propto 1/E$ is still valid.

Therefore, $E\Omega$ is independent of E and this suggests modifying the definition of the parameter R relevant to lifetime measurements such as

$$R = \frac{E_D \Omega(v_D \tau)}{E_P \Omega(v_P \tau)}. \quad (1)$$

For a given geometry of the experiment, R depends only on $v\tau$. Here v_D and v_P are the projections of the recoil velocity orthogonal to the axis in the delayed and prompt cases respectively. For the present geometry

$$\begin{aligned} v_D &\approx v \cos 3^\circ \approx v, \\ v_P &\approx v \sin 3^\circ \approx 0.05v \end{aligned} \quad (2)$$

In this way an energy-independent calibration curve is obtained.

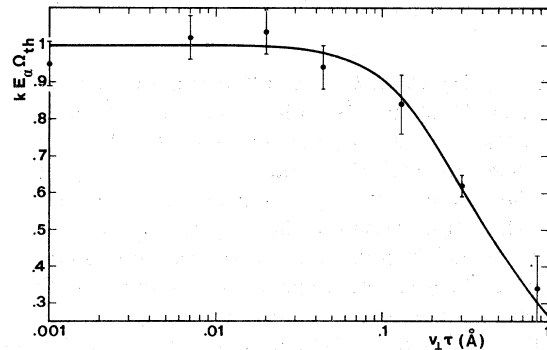


FIG. 8. Products $kE_\alpha \Omega_{th}$ vs $v_\perp \tau$ calculated for exponential decay with the Monte Carlo program. The best fit curve (see text) has parameters $k = 1.55 \pm 0.11 \text{ MeV}^{-1}$ and $\tau_c = 30 \pm 10 \text{ pm}$ (≈ 1.7 times the Thomas-Fermi screening length). The point at the origin is $kE_\alpha \Omega_{th}(v_\perp \tau = 0) = 1.01 \pm 0.04$. The volumes are calculated on a $\pi(17)^\circ \times 10^{-6} \text{ sr}$ solid angle. Error bars are only statistical.

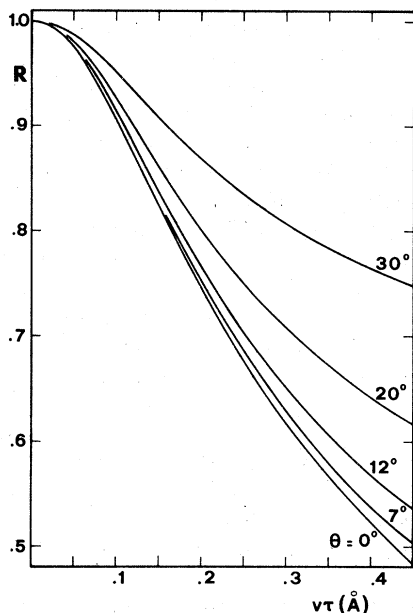


FIG. 9. Calibration curve $R(v\tau)$ constructed for different values of the angle θ between the beam and the $\langle 1\bar{1}0 \rangle$ axis (see Fig. 3). Data are from the best fit curve of Fig. 8.

B. Dependence of the parameter R on the mean displacement $v\tau$

To construct the calibration curve we carried out eight Monte Carlo calculations for different $v_{\perp}\tau$ ranging from 0 to 85 pm. The extracted products $E\Omega$ were connected by means of a fitting formula. Since $E\Omega$ has to be used in Eq. (1), it can be defined up to an arbitrary multiplicative constant k . If k is such that

$$\lim_{v_{\perp}\tau \rightarrow 0} kE\Omega = 1,$$

one can try to fit $kE\Omega$ as a function of $v_{\perp}\tau$ using "model 1" of Ref. 14, which contains a "cutoff interaction radius" r_c and does somehow take into account thermal vibrations.

The result of these calculations is shown in Fig. 8, where the values of the parameter k and r_c are also given. The volumes Ω are calculated on a cone of 17 mrad semiaperture, the same as that used for the experimental dips.

Figure 8 and Eq. (1) can be used to generate an explicit calibration curve $R(v\tau)$ for any experimental geometry. An example of such a procedure is shown in Fig. 9 for different values of the angle θ between the beam and the $\langle 1\bar{1}0 \rangle$ crystal axis (see Fig. 3). The curve $\theta = 3^\circ$ is not shown because it is indistinguishable from the $\theta = 0^\circ$ for $R \geq 0.5$.

No attempt has been made to evaluate the uncer-

tainties in the curves of Figs. 8 and 9 arising from the Monte Carlo procedure.

V. EXPERIMENTAL RESULTS

A. The 885-keV resonance

Two runs of 15 000 μC (I) and 20 000 μC (II) respectively were performed. The results are shown in Fig. 10. The χ_{min} value of the prompt dip ensures that the radiation damage is negligible and that there is no contribution from lower resonances since the corresponding dips would be filled by the depth effect.

The lifetime effect is particularly evident for run I both for the higher χ_{min} and the smaller width of the delayed dip. Owing to an alignment error, run II was performed at $\theta_{\text{lab}} = 83^\circ$ and 173° and cannot be directly compared with run I.

Table III summarizes the results for the 885-keV resonance. As always in this work the volumes correspond to a cone of 17 mrad semiaperture.

Transforming the result of run II to the same geometry of run I with the help of Fig. 9 gives an average

$$\langle R \rangle_{885} = 0.78 \pm 0.07 \quad (3)$$

corresponding to a mean displacement

$$(v\tau)_{885} = 18 \pm 4^5 \text{ pm}.$$

Hence

$$\tau_{885} = (38_{-9}^{+10}) \text{ as}. \quad (4)$$

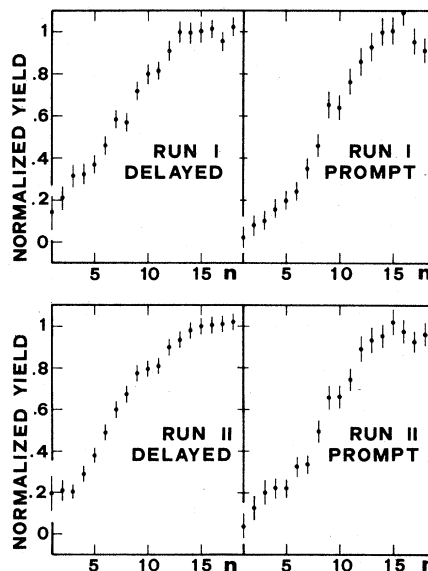


FIG. 10. Normalized experimental blocking dips found for the $E_p = 885\text{-keV}$ resonance. n is the ordering number of 1-mrad circular rings around the dip center.

TABLE III. Summary of the experimental results for the 885-keV resonance.

	Run I	Run II
E_D/E_P^a	1.103	1.109
Ω_D	0.159 ± 0.017	0.167 ± 0.014
Ω_P	0.226 ± 0.022	0.235 ± 0.018
R	0.776 ± 0.112	0.787 ± 0.090
$\langle R \rangle$	0.778 ± 0.070	
$v\tau$ (pm)	$17.7_{-1.8}^{+8}$	

^a E_D and E_P are calculated from the reaction kinematics and Q value (Ref. 3).

B. The 937-keV resonance

In this case five runs were made with five different crystals for a total of a 34 000 μC proton dose. A typical result is shown in Fig. 11. The delayed and prompt dips appear to be quite similar but, as pointed out in Sec. III C, no definite conclusion about the lifetime can be drawn before taking into account the contributions from the 923- and 885-keV resonances. The presence of these resonances (whose dips are also filled in by the depth effect) is made evident by the high χ_{min} and the flat bottom of the prompt dip.

From the definition of the dip volume it follows that the measured dip volume is a linear combination of the individual dip volumes:

$$\Omega_{\text{exp}} = c_{937}\Omega_{937} + c_{923}\Omega_{923} + c_{885}\Omega_{885}, \quad (5)$$

where the coefficients c_k are the yields of Table I, normalized as

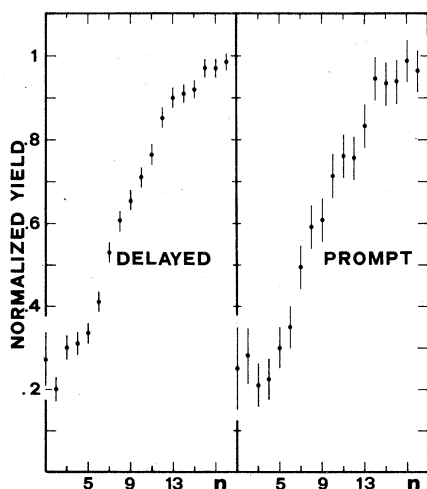


FIG. 11. Typical blocking dips found with a beam energy $E_p = 947$ keV. They correspond to a mixture of the 937-, 923-, 885-keV resonances.

$$\sum_{k=1}^3 c_k = 1. \quad (6)$$

Using Eqs. (5) and (6) and Table I, Ω_{937} has been calculated starting from Ω_{exp} and evaluating Ω_{923} and Ω_{885} as follows. These volumes were obtained from the Monte Carlo results (Fig. 8) corrected for the depth effect (Table II and Fig. 6). The assumed $v\tau$ were 85 pm (Ref. 4) for Ω_{923} and our result for Ω_{885} (see Sec. V A).

Repeating the calculations for each run gave mutually consistent values for Ω_D/Ω_P , so we took their weighted average to obtain the final result

$$R_{937} = 1.02 \pm 0.09, \quad (7)$$

which is compatible with zero lifetime. More precisely, from Fig. 9 one has

$$(v\tau)_{937} < 8.4 \text{ pm}.$$

Hence

$$\tau_{937} < 17 \text{ as}. \quad (8)$$

Quoted errors include the uncertainties in the yields of Table I and in the best fit line of Fig. 6. Neglecting the correction for the 923- and 885-keV resonances, R would be 0.89 ± 0.05 .

VI. CONCLUSIONS

We have measured the lifetimes of the 937- and 885-keV resonances in the $^{27}\text{Al}(p, \alpha)^{24}\text{Mg}$ reaction by the crystal blocking technique. We have used axial blocking, thick targets, and Kodak LR 115 type I (7 μm) cellulose nitrate detectors. The data were analyzed with reference to a multistring Monte Carlo model for the charged-particle motion through the crystal.

The 937-keV measurement was contaminated by two lower resonances. Their effect was accounted for by a detailed study of their yields and of the depth dependence of the blocking dips. After subtracting their contributions, we were not able to detect any lifetime effect and could only conclude that $\tau_{937} < 17$ as or $\Gamma_{937} > 39$ eV. This result agrees with that reported in the literature ($\Gamma = 130 \pm 15$ eV), but disagrees with the blocking experiment of Nakayama *et al.*⁵ The value reported there for the experimental R was, after correction for the 923-keV resonance, 0.95 ± 0.05 . It is not clear whether this result was obtained taking into account the energy and depth dependence of blocking dips, but in any case it appears to be compatible with zero lifetime and it seems to us that, with reference to Fig. 6 of Ref. 5, it would lead to $v\tau < 8$ pm, in good agreement with the present result.

In the 885-keV experiment we were able to discriminate the lower resonances using a 4 μm My-

TABLE IV. Comparison between present and previous results.

Authors	Method of measurement	Γ_{885} (eV)	Γ_{937} (eV)	Ref.
Alexander <i>et al.</i>	Axial blocking 0.1 μm	25_{-11}^{+19}		6
	Axial blocking 0.4 μm	14_{-3}^{+4}		6
Nakayama <i>et al.</i>	Planar blocking		60_{-20}^{+110} ^a	5
Maas <i>et al.</i>	(p, α) , (p, γ) , (α, γ) yields	12 ± 4 ^a	130 ± 15	4
Present exper.	Axial blocking 0.2 μm	17_{-4}^{+5}	>39	

^a For discussion see text, Sec. VI.

lar foil on the detectors. The measured lifetime is

$$\tau_{885} = 38_{-9}^{+10} \text{ as}$$

in fairly good agreement with the 0.1 μm blocking measurement of Alexander *et al.*⁶ that gives $\tau_{885} = 26_{-11}^{+18}$ as.

It must be noted that the value of the parameter R obtained in Ref. 6 is almost identical to the present one. The difference in the values of τ arises from the use of a different model to connect $\nu\tau$ to the measured R . In fact the curve which gives R vs $\nu\tau$ of Ref. 6 is obtained from analytical calculations based on the continuum model and does not take into account several effects, such as the lattice thermal vibrations, which, on the contrary, are properly accounted for in the Monte Carlo simulation.

The resonance width determined by the present experiment is $\Gamma_{885} = 17_{-4}^{+5}$ eV, in good agreement with the value 12 ± 4 eV obtained recently by Maas *et al.*⁴ from the (p, α) , (p, γ) , and (α, γ) yields. As suggested by Endt,¹⁷ here the most questionable point is the (p, γ) yield, which in Ref. 4 was taken from the work of Meyer *et al.*¹⁵ If, however, the (p, γ) data of Lyons *et al.*¹⁶ were used, a 40%

larger value for Γ_{885} would be found,¹⁷ in nearly perfect agreement with the present result. The results of the present experiment are summarized together with existing literature data in Table IV.

Further blocking studies on other $^{27}\text{Al}(p, \alpha)$ resonances and a more careful investigation into the difference of the results and the method of analysis between this work and Ref. 6 could lead to a better understanding of the validity of this method for measuring nuclear reaction times. This is probably necessary before attempting to use blocking for detailed studies of nuclear structure.

Further measurements on the 731-keV resonance are in progress and will be reported on completion.

We thank D. Bulgarelli and A. Grilli for their invaluable help during this work, and P. Kustatscher and the entire staff of the Laboratori Nazionali di Legnaro for the very efficient running of the 2-MeV Van de Graaff accelerator. The technical assistance of G. Laurenti and the mechanical workshop of our Institute are gratefully acknowledged. We are also deeply indebted to Professor P. M. Endt for help in discussing our results, and to Professor E. Rimini for useful information.

¹See, for instance, W. M. Gibson, *Annu. Rev. Nucl. Sci.* **25**, 465 (1975), and references therein.

²K. Yazaki and S. Yoshida, *Nucl. Phys.* **A232**, 249 (1974); S. Yoshida, *Annu. Rev. Nucl. Sci.* **24**, 1 (1974); F. Malaguti, A. Uguzzoni, and E. Verondini, *Lett. Nuovo Cimento* **2**, 629 (1971); E. P. Kanter, D. Koll-ewe, K. Komaki, I. Leuca, G. M. Temmer, and W. M. Gibson, *Nucl. Phys.* **A299**, 230 (1978).

³R. P. Sharma, J. U. Andersen, and K. O. Nielsen, *Nucl. Phys.* **A204**, 371 (1973).

⁴P. M. Endt and C. Van der Leun, *Nucl. Phys.* **A214**, 202 (1973); **A214**, 205 (1973); J. W. Maas, E. Somorjai, H. D. Graber, C. A. Van Den Wijngaart, C. Van der

Leun, and P. M. Endt, *ibid.* **A301**, 213 (1978).

⁵H. Nakayama, M. Ishii, K. Hisataka, F. Fujimoto, and K. Komaki, *Nucl. Phys.* **A208**, 545 (1973).

⁶R. B. Alexander, J. U. Andersen, and K. G. Prasad, *Nucl. Phys.* **A279**, 278 (1977).

⁷F. Malaguti, A. Uguzzoni, and E. Verondini, *Radiat. Eff.* **32**, 109 (1977).

⁸J. F. Ziegler and W. K. Chu, *At. Data Nucl. Data Tables* **13**, 463 (1974); W. Whaling, in *Encyclopedia of Physics*, edited by S. Flügge (Springer, Berlin, 1958), Vol. 34, p. 193.

⁹L. C. Northcliffe and R. F. Schilling, *Nucl. Data Tables* **A7**, 233 (1970).

- ¹⁰*Applications of Ion Beams to Metals*, edited by S. T. Picraux, E. P. EerNisse, and F. L. Vook (Plenum, New York, 1974), Chap. 7. The blistering effect might be related to the dimpling observed in thin crystal under irradiation by R. L. Meek, W. M. Gibson, and J. P. F. Sellschop, *Radiat. Eff.* 11, 139 (1971).
- ¹¹G. Foti, F. Grasso, R. Quattrocchi, and E. Rimini, *Phys. Rev. B* 3, 2169 (1971).
- ¹²E. Fuschini, F. Malaguti, C. Maroni, I. Massa, A. Uguzzoni, E. Verondini, and G. J. Clark, *Nuovo Cimento* 10A, 177 (1972).
- ¹³J. Lindhard, *K. Dan. Vidensk. Selsk. Mat. Fys. Medd.* 34, No. 14 (1965), Eq. (6.9).
- ¹⁴F. Malaguti and E. Verondini, *Nuovo Cimento* 28A, 240 (1975).
- ¹⁵M. A. Meyer, I. Venter, and D. Reitmann, *Nucl. Phys.* A250, 235 (1975).
- ¹⁶P. B. Lyons, J. W. Toevs, and D. G. Sargood, *Nucl. Phys.* A130, 1 (1969).
- ¹⁷P. M. Endt, private communication.